

# Fixed energy potentials through an auxiliary inverse eigenvalue problem

Tamás Pálmai and Barnabás Apagyi

Department of Theoretical Physics, Institute of Physics

Budapest University of Technology and Economics

H-1111 Budafoki út 8, Budapest, Hungary

palmai@phy.bme.hu

February 10, 2012

## Abstract

An inverse scattering method based on an auxiliary inverse Sturm-Liouville problem recently proposed by Horváth and Apagyi [Mod. Phys. Lett. B 22, 2137 (2008)] is examined in various aspects and developed further to (re)construct spherically symmetric fixed energy potentials of compact support realized in the three-dimensional Schrödinger equation. The method is generalized to obtain a family of inverse procedures characterized by two parameters originating, respectively, from the Liouville transformation and the solution of the inverse Sturm-Liouville problem. Both parameters affect the bound states arising in the auxiliary inverse spectral problem and one of them enables to reduce their number which is assessed by a simple method. Various solution techniques of the underlying moment problem are proposed including exact Cauchy matrix inversion method, usage of spurious bound state and assessment of the number of bound states. Examples include (re)productions of potentials from phase shifts known theoretically or derived from scattering experiments.

PACS: 02.30.Zz, 02.60.Cb, 02.60.Pn, 03.65.Nk

AMS subject classification: 34L25, 65L09, 81U40

## 1 Introduction

We consider the three-dimensional inverse scattering problem of the Schrödinger equation on the half-line at a fixed scattering energy [1, 2]. For spherically symmetric potentials the partial wave expansion applies and the radial Schrödinger equations

$$r^2 \left[ -\frac{d^2}{dr^2} + q(r) - k^2 \right] \varphi_l(r) = -l(l+1)\varphi_l(r), \quad l = 0, 1, 2, \dots \quad (1)$$

with the physical boundary conditions describe the scattering of two non-relativistic quantum mechanical objects (potential scattering). Presently  $k$  is fixed to a constant value and we assume that  $q(r)$  is compactly supported, i.e.  $q(r) = 0$  for  $r \geq a$ . Moreover we require that

$$rq(r) \in L^1(0, a). \quad (2)$$

For this problem it can be shown that

$$\varphi_l(r) = C_l r^{l+1} (1 + o(1)), \quad r \rightarrow 0, \quad (3)$$

$$\varphi_l(r) = A_l \sqrt{r} \left( J_{l+1/2}(kr) - \tan \delta_l Y_{l+1/2}(kr) \right), \quad r \geq a, \quad (4)$$

where the phase shifts  $\delta_l$  arise.

In [3] it was shown that a subset of the fixed energy phase shifts, whose indices satisfy the Müntz condition, determines the m-function and thus the spectral function, and thereby the potential of an auxiliary inverse eigenvalue problem (i.e. an inverse Sturm-Liouville problem). Based on this proof a constructive method was suggested in [4] for the solution of the inverse scattering problem at fixed energy.

In this paper we develop this method further by generalizing both the transformation of the fixed energy inverse scattering problem to the inverse spectral problem and the constructive inversion method of the inverse eigenvalue problem. In [4] only the case when one bound state is present in the auxiliary problem has been addressed. We examine the zero and the multiple bound state cases. In the latter one we find that it involves a highly nonlinear system of equations which is difficult to solve. One way to overcome the difficulties would be to reduce the number of bound states and to leave the nonlinear regime. Remarkably, this can be achieved in many cases by tuning the parameters found by the generalization of the original method. Also, an approximative argument is presented to assess the number of bound states present in the auxiliary problem.

The paper is structured as follows: in the next section the transformation of the fixed energy inverse scattering problem is generalized. Section 3 contains a brief summary of the classical inverse Sturm-Liouville theory and the utilization thereof in the present problem. In section 4 solution methods of the inverse problem at different bound state levels are discussed. In section 5 an approximative method is given to determine the number of bound states and also the possibility to reduce their number is studied. Section 6 is devoted to illustrative applications, section 7 is left for a summary.

## 2 Liouville transformation

First the fixed energy problem is transformed to an inverse eigenvalue problem where the value of the m-function for some arguments is determined from the original fixed energy phase shifts. To this end we transform the radial Schrödinger equation (1) to the Liouville normal form (see e.g. [5]) by using a Liouville transformation,

$$r \rightarrow x(r), \quad \varphi_l(r) \rightarrow \psi_l(x). \quad (5)$$

Rewriting the differential equation (1) in terms of the new independent variable  $x$  and dependent variable  $\psi_l(x) = f(x)^{-1} \varphi_l(r(x))$  yields

$$-\psi_l''(x) - \left[ \frac{\ddot{x}}{\dot{x}^2} + 2 \frac{f'(x)}{f(x)} \right] \psi_l'(x) + \left[ \frac{q(r(x)) - k^2}{\dot{x}^2} - \frac{\ddot{x}}{\dot{x}^2} \frac{f'(x)}{f(x)} - \frac{f''(x)}{f(x)} \right] \psi_l(x) = -\frac{l(l+1)}{r(x)^2 \dot{x}^2} \psi_l(x) \quad (6)$$

where dot denotes differentiation with respect to  $r$ . To get the Liouville normal form of the Sturm-Liouville equation we need

$$r(x)^2 \dot{x}^2 = \text{const.} = c^2, \quad (7)$$

and

$$\left[ \frac{\ddot{x}}{\dot{x}^2} + 2 \frac{f'(x)}{f(x)} \right] \equiv 0. \quad (8)$$

The two conditions yield the unique solution

$$x(r) = c \log r + c_1 \quad (9)$$

and

$$f(x) = c_2 e^{\frac{x}{2c}}. \quad (10)$$

If we want to use the inverse spectral theory of the Sturm-Liouville equation on  $(0, \infty)$  we need  $x(0) = +\infty$  and  $x(a) = 0$  which in turn implies

$$\operatorname{sgn} c = -1, \quad c_1 = -c \log a. \quad (11)$$

Without the loss of generality  $c_2 = 1$  is set and then the only remaining parameter  $c$  can be chosen arbitrarily maintaining the negative sign.

In summary we have only one family of Liouville transformations reducing the radial Schrödinger equation (1) to the Liouville normal form, namely

$$x(r) = c \log \frac{r}{a}, \quad c < 0, \quad (12)$$

$$\psi_l(x) = e^{-\frac{x}{2c}} \varphi_l(ae^{\frac{x}{c}}). \quad (13)$$

Thereby (1) transforms to

$$-\psi_l''(x) + Q(x)\psi_l(x) = -\frac{1}{c^2} \left(l + \frac{1}{2}\right)^2 \psi_l(x), \quad (14)$$

with the auxiliary potential

$$Q(x) = \frac{a^2}{c^2} e^{\frac{2x}{c}} (q(ae^{\frac{x}{c}}) - k^2). \quad (15)$$

The transformed equation can be viewed as

$$S[Q(x)]y(x, \lambda) = \lambda y(x, \lambda), \quad S[Q(x)] = -\frac{d^2}{dx^2} + Q(x) \quad (16)$$

given explicitly at

$$\lambda = -\frac{1}{c^2} \left(l + \frac{1}{2}\right)^2 \quad (17)$$

also obtaining one of the two linearly independent solutions of the Sturm-Liouville equation as

$$y \left( x, -\frac{1}{c^2} \left(l + \frac{1}{2}\right)^2 \right) = \psi_l(x). \quad (18)$$

(Later we show that this is an  $L^2$  solution.)

Note that in the original Horváth-Apagyi [4] method  $c = -1$  was taken implicitly.

### 3 Inverse Sturm-Liouville problem

#### 3.1 Summary of the classical inverse Sturm-Liouville problem

**Spectral properties** For the Sturm-Liouville equation

$$-y_\alpha''(x, \lambda) + Q(x)y_\alpha(x, \lambda) = \lambda y_\alpha(x, \lambda), \quad x \in [0, \infty) \quad (19)$$

with the initial conditions

$$y_\alpha(0, \lambda) = \sin \alpha \neq 0, \quad y'_\alpha(0, \lambda) = -\cos \alpha, \quad (20)$$

there exists [6, 7] a monotone increasing function  $\rho_\alpha(\lambda)$ , the *spectral function*, such that, for every  $f(x) \in L^2(0, \infty)$  there exists in the  $L^2(-\infty, \infty, \rho_\alpha(\lambda))$  norm sense

$$F_\alpha(\lambda) = \text{l.i.m.}_{n \rightarrow \infty} \int_0^n f(x) y_\alpha(x, \lambda) dx \quad (21)$$

and this is a unitary transformation, i.e. the Parseval formula

$$\int_0^\infty |f(x)|^2 dx = \int_{-\infty}^\infty |F_\alpha(\lambda)|^2 d\rho_\alpha(\lambda) \quad (22)$$

holds (a theorem of Weyl).

A property of the spectral function is the formula [6, 7]

$$\rho_\alpha(\lambda) = \frac{2}{\pi \sin^2 \alpha} \lambda^{1/2} + \rho_\alpha(-\infty) + \frac{\cos \alpha}{\sin^3 \alpha} + o(1), \quad \lambda \rightarrow \infty. \quad (23)$$

If  $Q(x) \in L^1(0, \infty)$  then the Sturm-Liouville operator is in the limit-point case at infinity and the *Weyl-Titchmarsh m-function* is defined uniquely by

$$m(\lambda) = \frac{y'(0, \lambda)}{y(0, \lambda)} \quad (24)$$

where  $y(x, \lambda)$  is a solution belonging to the function space  $L^2(0, \infty)$ .

The m-function is related to the spectral function through a certain kind of Stieltjes transform [6]

$$\frac{\sin \alpha - m(\lambda) \cos \alpha}{\cos \alpha + m(\lambda) \sin \alpha} = -\cot \alpha + \int_{-\infty}^\infty \frac{d\rho_\alpha(t)}{\lambda - t}. \quad (25)$$

An equivalent formulation is given for the solution of the Sturm-Liouville equation with the initial conditions

$$y^h(0, \lambda) = 1, \quad y^{h'}(0, \lambda) = h < \infty. \quad (26)$$

Prescribing  $h = -\cot \alpha$  one has  $[\sin \alpha y^h](0, \lambda) = \sin \alpha$  and  $[\sin \alpha y^h]'(0, \lambda) = -\cos \alpha$  thus  $\sin \alpha y^h(x, \lambda) = y_\alpha(x, \lambda)$ . Then  $F_\alpha(\lambda) = \sin \alpha \int_0^\infty f(x) y^h(x, \lambda) dx = \sin \alpha F^h(\lambda)$  for  $f(x) \in L^2(0, \infty)$  in the norm sense. The Parseval formula (22) yields

$$\rho^h(\lambda) = \rho_\alpha(\lambda) \sin^2 \alpha. \quad (27)$$

$\rho^h(\lambda)$  is related to the m-function by

$$\frac{1}{m(\lambda) - h} = \int_{-\infty}^\infty \frac{d\rho^h(t)}{\lambda - t}, \quad (28)$$

which formula can be inverted by the Stieltjes inversion (see e.g. XIV. §3. of [7])

$$\rho^h(\lambda_2) - \rho^h(\lambda_1) = -\frac{1}{\pi} \lim_{\varepsilon \rightarrow 0^+} \int_{\lambda_1}^{\lambda_2} \text{Im} \frac{1}{m(\lambda + i\varepsilon) - h} d\lambda. \quad (29)$$

One can see that the two formulations are completely equivalent. We will use the latter one since it is traditionally used in the Gel'fand-Levitan construction discussed below.

We note that in the original formalism of Horváth and Apagyi [4]  $h = 0$  was taken implicitly.

**Construction of the potential from the spectral function** From the existence of the spectral function the Gel'fand-Levitan (GL) integral equation can be deduced [6]:

$$0 = F(x, t) + K(x, t) + \int_0^x K(x, s)F(s, t)ds \quad (0 \leq t \leq x), \quad (30)$$

where the input symmetrical kernel is

$$F(x, t) = \int_{-\infty}^{\infty} \cos(\sqrt{\lambda}x) \cos(\sqrt{\lambda}t) d\sigma(\lambda) = \frac{1}{2}(F(x+t) + F(|x-t|)), \quad (31)$$

$$F(x) = \int_{-\infty}^{\infty} \cos(\sqrt{\lambda}x) d\sigma(\lambda), \quad \sigma(\lambda) = \rho^h(\lambda) - \rho^{0,0}(\lambda). \quad (32)$$

$\rho^h(\lambda)$  is defined as before while  $\rho^{0,0}(\lambda)$  is the spectral function for the zero potential with boundary conditions  $y(0) = 1$ ,  $y'(0) = 0$ , i.e.,

$$\rho^{0,0}(\lambda) = \begin{cases} \frac{2}{\pi}\sqrt{\lambda}, & \lambda \geq 0 \\ 0, & \lambda < 0. \end{cases} \quad (33)$$

In the GL equation  $K(x, y)$  is the kernel of the transformation operator  $T_{Q,0} : L^2 \rightarrow L^2$  realized as

$$T_{Q,0}f(x) = f(x) + \int_0^x K(x, t)f(t)dt, \quad T_{Q,0}y_{0,0}(x, \lambda) = y_{Q,h}(x, \lambda) \quad (34)$$

mapping the solutions of the Sturm-Liouville equation with  $Q \equiv 0$  satisfying the boundary conditions

$$f(0) = 1, \quad f'(0) = 0, \quad (35)$$

onto the solutions with  $Q \neq 0$  satisfying

$$f(0) = 1, \quad f'(0) = h < \infty. \quad (36)$$

The transformation kernel is connected to the potential  $Q(x)$  by

$$Q(x) = 2 \frac{d}{dx} K(x, x). \quad (37)$$

### 3.2 m-function of the operator $S[Q(x)]$

First we show that for the above-defined potential  $Q(x)$ ,  $Q(x) \in L^1(0, \infty)$  holds:

$$\int_0^\infty |Q(x)|dx \leq \frac{1}{c^2} \int_0^a r^2 |q(r)|dr + \frac{a^2 k^2}{2|c|} < \infty \quad (38)$$

by equation (2), the fact that  $\int_0^a r^2 |q(r)|dr < a \int_0^a r |q(r)|dr$  and  $c < 0$  was employed. Then  $S[Q(x)]$  with  $Q(x)$  being the auxiliary potential is in the limit-point case.

Next we prove that the functions  $\{\psi_l(x)\}_{l=0,1,\dots}$  are of the class  $L^2(0, \infty)$ :

$$\int_0^\infty |\psi_l(x)|^2 dx = \int_0^\infty e^{-\frac{x}{c}} |\varphi_l(ae^{\frac{x}{c}})|^2 dx = a|c| \int_0^a \frac{|\varphi_l(r)|^2}{r^2} dr < \infty, \quad (39)$$

where  $l \geq 0$  was exploited and the asymptotic formula  $\varphi(r) = Cr^{l+1}(1 + o(1))$ ,  $r \rightarrow 0$  coming from equation (3) was used to estimate the integral.

Since  $\psi_l(x) \in L^2(0, \infty)$  and  $Q(x) \in L^1(0, \infty)$  we infer that the m-function of the Sturm-Liouville operator  $S[Q(x)]$  satisfies

$$m\left(-\frac{(l+1/2)^2}{c^2}\right) = \frac{\psi'_l(0)}{\psi_l(0)} = \frac{ka}{c} \frac{J'_{l+1/2}(ka) - \tan \delta_l Y'_{l+1/2}(ka)}{J_{l+1/2}(ka) - \tan \delta_l Y_{l+1/2}(ka)}. \quad (40)$$

From this we can build the potential through the formula relating the m-function to the spectral function and the constructive method discussed previously.

### 3.3 Deriving a moment problem

With reference to the defining formula (32) for  $F(x)$  we define a truncated version  $\tilde{F}(x)$ :

$$\tilde{F}(x) = \int_0^\infty \cos(\sqrt{\lambda}x) d\sigma(\lambda). \quad (41)$$

It turns out that the reconstruction of the  $\tilde{F}(x)$  function from the given m-function values is an inverse moment problem. Consider

$$I = \int_0^\infty \tilde{F}(x) e^{(l+\frac{1}{2})\frac{x}{c}} dx = \int_0^\infty \int_0^\infty d\sigma(\lambda) dx \cos(\sqrt{\lambda}x) e^{(l+\frac{1}{2})\frac{x}{c}} = -\frac{1}{c} \int_0^\infty d\sigma(\lambda) \frac{l + \frac{1}{2}}{\frac{1}{c^2} (l + \frac{1}{2})^2 + \lambda}. \quad (42)$$

This integration can be performed with ease in terms of the m-function and by considering that on  $(-\infty, 0)$   $d\rho^h(\lambda)$  is concentrated at the bound states  $\lambda_1, \dots, \lambda_B$  supported by  $S[Q(x)]$ :

$$I = \frac{1}{c} \left( l + \frac{1}{2} \right) \left[ \int_{-\infty}^\infty \frac{d(\rho^h(\lambda) - \rho^{0,0}(\lambda))}{-\frac{1}{c^2} (l + \frac{1}{2})^2 - \lambda} + \int_{-\infty}^0 \frac{d\rho^h(\lambda)}{\frac{1}{c^2} (l + \frac{1}{2})^2 + \lambda} \right] \quad (43)$$

$$= \frac{1}{c} \left( l + \frac{1}{2} \right) \left[ \frac{1}{m \left( -\frac{1}{c^2} (l + \frac{1}{2})^2 \right) - h} - \frac{1}{m_0 \left( -\frac{1}{c^2} (l + \frac{1}{2})^2 \right)} + \sum_{i=1}^B \frac{b_i}{\frac{1}{c^2} (l + \frac{1}{2})^2 + \lambda_i} \right]. \quad (44)$$

Here

$$b_i = \rho^h(\lambda_i + 0) - \rho^h(\lambda_i - 0) \quad (45)$$

and  $m_0(\cdot)$  denotes the m-function associated with  $Q(x) \equiv 0$ . The values of  $m(\cdot)$  appearing in (44) are determined by (40). For a more detailed derivation consult [4].

Now we have the following problem for the truncated  $\tilde{F}(x)$ :

$$\int_0^\infty \tilde{F}(x) e^{(l+\frac{1}{2})\frac{x}{c}} dx = \mu(c, h, \delta_l, \{\lambda_i\}, \{b_i\}), \quad l = 0, 1, \dots \quad (46)$$

with the moments (assuming  $B$  bound states)

$$\begin{aligned} \mu(c, h, \delta_l, \{\lambda_i\}, \{b_i\}) = & \left( l + \frac{1}{2} \right) \left( ka \frac{J'_{l+1/2}(ka) - \tan \delta_l Y'_{l+1/2}(ka)}{J_{l+1/2}(ka) - \tan \delta_l Y_{l+1/2}(ka)} - c h \right)^{-1} - 1 \\ & + \sum_{i=1}^B \frac{\frac{b_i}{c} (l + \frac{1}{2})}{\frac{1}{c^2} (l + \frac{1}{2})^2 + \lambda_i}, \end{aligned} \quad (47)$$

which is essentially a moment problem. Note that unless there are no bound states the moments depend on the undetermined quantities  $\{\lambda_i\}$  and  $\{b_i\}$  associated to the bound state positions and norms.

## 4 Solution method

Depending on the number of bound states present in the auxiliary problem, different solution strategies are called for. As a consequence it is important to know or assess the number of bound states before solving the inverse problem which is discussed in the next section.

## 4.1 No bound states

In this case we have a proper moment problem for  $\tilde{F}(x) = F(x)$ :

$$\int_0^\infty F(x) e^{(l+\frac{1}{2})\frac{x}{c}} dx = \mu(c, h, \delta_l) \equiv \mu_l, \quad (48)$$

where the moments now do not depend on unknown quantities.

To solve this moment problem we use the following expansion for  $F(x)$ :

$$F(x) = \sum_{n=0}^N c_n e^{-nx}. \quad (49)$$

Upon substitution into equation (48) and using  $N + 1$  fixed energy phase shifts as input data we get the following system of linear equations for the coefficients:

$$\sum_{n=0}^N c_n \frac{-c}{-cn + l + \frac{1}{2}} = \mu_l, \quad l = 0, 1, \dots, N. \quad (50)$$

Solving this system of linear equations yield the coefficients required to build  $F(x)$  and from that one can calculate the fixed energy potential essentially by solving the GL integral equation (30). Note that solving the system of equations is not a well-conditioned task as we must deal with a Hilbert-type matrix which is infamously badly conditioned. Therefore, from the numerical point of view it is of considerable value to see, that this matrix can be inverted explicitly. Our matrix, i.e.  $\left[ \frac{-c}{-cn+l+\frac{1}{2}} \right]_{ln}$  is in fact a Cauchy matrix. The elements of the inverse of a general Cauchy matrix with elements  $a_{ij} = (x_i + y_j)^{-1}$  are given by [9]

$$b_{ij} = (x_j + y_i) \prod_{m \neq i} \frac{x_j + y_m}{y_m - y_i} \prod_{m \neq j} \frac{x_m + y_i}{x_m - x_j}. \quad (51)$$

In our case this implies

$$c_n = -\frac{1}{c} \sum_{l=0}^N \mu_l \left( l - cn + \frac{1}{2} \right) \prod_{n' \neq n} \frac{l - cn' + \frac{1}{2}}{cn - cn'} \prod_{l' \neq l} \frac{l' - cn + \frac{1}{2}}{l' - l}, \quad n = 0, 1, \dots, N. \quad (52)$$

**Improvements of the solution method** To further improve the solution method outlined above one can exploit two properties of the  $F(x)$  function, namely that

$$F(0) = -h, \quad (53)$$

$$\lim_{x \rightarrow \infty} F(x) = 0. \quad (54)$$

The latter is a simple consequence of the Riemann-Lebesgue lemma, however the former needs more explanation. Let us write up

$$\begin{aligned} F(0) &= \int_{-\infty}^{\infty} d\sigma(\lambda) = \lim_{\Lambda \rightarrow \infty} \int_{-\infty}^{\Lambda} d\sigma(\lambda) = \lim_{\Lambda \rightarrow \infty} \left[ \rho^h(\Lambda) - \rho^h(-\infty) - \frac{2}{\pi} \sqrt{\Lambda} \right] = \\ &= \lim_{\Lambda \rightarrow \infty} \left[ \frac{2}{\pi} \sqrt{\Lambda} + \rho^h(-\infty) - h + o(1) - \rho^h(-\infty) - \frac{2}{\pi} \sqrt{\Lambda} \right] = -h \end{aligned} \quad (55)$$

where equation (23) was used and continuity in  $\Lambda$  was supposed. This proves  $F(0) = -h$ .

Because of  $F(\infty) = 0$  one can take

$$c_0 = 0; \quad (56)$$

however, we note that this is not always the best course of action in practical scenarios (see Examples).

To incorporate the information  $F(0) = -h$  there are several ways to choose from. For instance, one can prescribe the condition

$$\sum_{n=0}^N c_n = -h \quad (57)$$

for the coefficients (which complicates the solution process: the matrix to be inverted is no longer of the Cauchy type). On the other hand, this will be very useful in the one bound state case (see later) where it will permit to determine the nonlinear parameter  $\lambda$  in a linear way.

**Hausdorff moment problem** Our problem can be viewed as a Hausdorff moment problem since with  $z = e^{\frac{x}{c}}$  and  $\mathfrak{F}(z) = -cz^{-1/2}F(c \log z)$  (48) takes the form

$$\int_0^1 z^l \mathfrak{F}(z) dz = \mu_l, \quad l = 0, 1, 2, \dots \quad (58)$$

The Hausdorff moment problem is studied in the literature in detail concerning both mathematical properties and solution methods. For instance, an interesting stability result can be found in [10] whose corollary is the following theorem. It establishes an accuracy estimate of the inverse moment problem which is procedure independent.

**Theorem 1.** *Suppose the smoothness condition*

$$\int_0^1 |\mathfrak{F}'(z) - \mathfrak{F}'_N(z)|^2 dz \leq E^2 < \infty. \quad (59)$$

*Then if the first  $N + 1$  moments of  $\mathfrak{F}(z)$  and  $\mathfrak{F}_N(z)$  coincide, i.e.*

$$\int_0^1 z^k \mathfrak{F}(z) dz = \int_0^1 z^k \mathfrak{F}_N(z) dz, \quad k = 0, 1, \dots, N, \quad (60)$$

*we have*

$$\int_0^1 |\mathfrak{F}(z) - \mathfrak{F}_N(z)|^2 dz \leq \frac{E^2}{4(N+1)^2}. \quad (61)$$

Using Theorem 1 one can conclude that if the moments  $\mu_l$  are free of error, the difference between the approximated and the true  $F(x)$  functions in  $L^2$  norm tends to 0 as the number of moments is increased:

$$\int_0^\infty |F(x) - F_N(x)|^2 dx \leq \frac{C}{4(N+1)^2}, \quad (62)$$

with some  $C$  constant depending on the smoothness of  $F(x) - F_N(x)$ ,

$$\int_0^\infty |F'(x) - F'_N(x)|^2 e^{-\frac{2x}{c}} dx \leq C, \quad (63)$$

and  $F_N(x)$  is the approximation of the true  $F(x)$  using the first  $N + 1$  moments.

It is interesting to consider the case when the input data is noisy. Using Theorem 1 of [10] one can state the following:

$$\int_0^\infty |F(x) - F_N(x)|^2 dx \leq \min_n \left\{ \frac{\varepsilon^2}{|c|} e^{3.5(n+1)} + \frac{C}{4(n+1)^2} : n = 0, 1, \dots, N \right\}, \quad (64)$$

where  $\varepsilon^2$  is the absolute square sum of the differences between the true and noisy moments. This result implies in particular that even if the number of phase shifts grows to infinity the recovery will not be complete when the data remains erroneous.



## 4.2 One bound state

Supposing (49) we get the system of equations

$$\sum_{n=0}^N c_n \frac{-c}{-cn + l + \frac{1}{2}} = \mu_l + \frac{b(l + \frac{1}{2}) \frac{1}{c}}{\frac{1}{c^2}(l + \frac{1}{2})^2 + \lambda}, \quad l = 0, 1, \dots, N+1, \quad (65)$$

where  $\mu_l$  denotes the  $l$ th moment without the bound state contributions and  $\lambda < 0$  and  $b > 0$  are the bound state parameters (the subscript 1 is omitted). Using the expansion (49) for  $\tilde{F}(x)$  we have

$$F(x) = b \cosh(\sqrt{-\lambda}x) + \sum_{n=0}^N c_n e^{-nx}. \quad (66)$$

To get an explicitly solvable system of equations treating  $\sqrt{-\lambda}$  as a parameter we subtract the term  $\frac{b}{2}e^{-\sqrt{-\lambda}x}$  from the expansion for  $\tilde{F}(x)$ , that is

$$\tilde{F}(x) = \sum_{n=0}^N c_n e^{-nx} - \frac{b}{2}e^{-\sqrt{-\lambda}x}, \quad F(x) = \frac{b}{2}e^{\sqrt{-\lambda}x} + \sum_{n=0}^N c_n e^{-nx}, \quad (67)$$

and obtain

$$\frac{-cb}{2((l + \frac{1}{2}) + c\sqrt{-\lambda})} + \sum_{n=0}^N c_n \frac{-c}{-cn + l + \frac{1}{2}} = \mu_l, \quad l = 0, 1, \dots, N+1 \quad (68)$$

through the elementary identity

$$\frac{\alpha}{\alpha^2 - \beta^2} - \frac{1}{2} \frac{1}{(\alpha + \beta)} = \frac{1}{2} \frac{1}{\alpha - \beta}, \quad \alpha, \beta \in \mathbb{C}. \quad (69)$$

The explicit solution of the system of equations is given by

$$c_n = -\frac{1}{c} \sum_{l=0}^{N+1} \mu_l \left( l - cn + \frac{1}{2} + c\delta_{n,-1}\sqrt{-\lambda} \right) \prod_{n' \neq n} \frac{l - cn' + \frac{1}{2} + c\delta_{n',-1}\sqrt{-\lambda}}{-cn' + c\delta_{n',-1}\sqrt{-\lambda} + cn - c\delta_{n,-1}\sqrt{-\lambda}} \times \prod_{l' \neq l} \frac{l' - cn + \frac{1}{2} + c\delta_{n,-1}\sqrt{-\lambda}}{l' - l}, \quad (70)$$

where  $n = -1$  is also allowed,  $c_{-1} \equiv \frac{b}{2}$  and  $\delta_{a,b}$  is the Kronecker-delta. To determine  $\sqrt{-\lambda}$  we use a result concerning Cauchy matrices, namely that the sum of the coefficients (including  $b/2$ ) is linear in  $\sqrt{-\lambda}$  (see e.g. [4], Lemma 5):

$$S = \sum_{n=-1}^N c_n = \alpha\sqrt{-\lambda} + \beta. \quad (71)$$

Using this fact the linear solution procedure is performed as follows.

1. Calculate  $S$  for two arbitrarily chosen  $\lambda$  values ( $\lambda_{01}$  and  $\lambda_{02}$ ) solving (68). Denoting the two sums  $S_1$  and  $S_2$ , using the relation  $S = F(0) = -h$  get  $\sqrt{-\lambda}$  by

$$\sqrt{-\lambda} = \frac{(S_2 + h)\sqrt{-\lambda_{01}} - (S_1 + h)\sqrt{-\lambda_{02}}}{S_2 - S_1}. \quad (72)$$

2. Calculate the  $c_n$  coefficients from (68) with the appropriate  $\lambda$  parameter obtained in (i).
3. Calculate  $q(r)$  through  $F(x)$  and the GL integral equation.

### 4.3 Multiple bound states

For two or more bound states we propose a non-linear problem as follows.

1. Solve the nonlinear system of equations

$$\sum_{i=1}^B \frac{-c b_i}{2(l + \frac{1}{2} + c\sqrt{-\lambda_i})} + \sum_{n=0}^N c_n \frac{-c}{-cn + l + \frac{1}{2}} = \mu_l, \quad l \in L \quad (73)$$

$$\sum_{i=1}^B b_i + \sum_{n=0}^N c_n = -h \quad (74)$$

with the index set  $L = [0, 1, \dots, N + 2B - 1]$  in the variables  $\lambda_1, \lambda_2, \dots, \lambda_B, b_1, b_2, \dots, b_B, c_0, c_1, \dots, c_N$ .

2. Calculate  $F(x)$  by

$$F(x) = \sum_{i=1}^B \frac{b_i}{2} e^{\sqrt{-\lambda_i}x} + \sum_{n=0}^N c_n e^{-nx}. \quad (75)$$

3. Solve the GL integral equation to obtain the potential.

Numerically, it is worthwhile to initialize the variables for the nonlinear solver with the ones obtained supposing a vanishing potential  $q(r) \equiv 0$ . This is because, roughly speaking,  $q(r)$  is expected to influence only the tail of the  $Q(x)$  potential and the bound states shall be close to those corresponding to  $q(r) \equiv 0$  (see next section).

## 5 Assessment of bound states

We shall make observations based on the transformation formula for the potential (15):

$$Q(x) = \frac{a^2}{c^2 e^{\frac{2x}{|c|}}} \left[ q(ae^{-\frac{x}{|c|}}) - k^2 \right], \quad q(a) = 0. \quad (76)$$

No bound state is expected when  $q(r) > k^2$  on  $0 \leq r < a$ , that is when  $Q(x)$  is positive everywhere, at least for  $h = 0$ . This is the case, for example, when we have a constant fixed-energy  $q(r)$  potential in the form

$$q(r) = \begin{cases} C & \text{for } r < a, \\ 0 & \text{for } r \geq a, \end{cases} \quad C > k^2. \quad (77)$$

However, in practical applications it is a far more natural assumption that  $q(r) = 0$  already on  $b < r < a$  with some  $b > 0$ . In this case we have

$$Q(x) = - \left( \frac{ka}{c} \right)^2 e^{-2\frac{x}{|c|}}, \quad 0 \leq x < -|c| \log \left( \frac{b}{a} \right), \quad (78)$$

and only the tail of  $Q(x)$  is influenced by the fixed-energy potential  $q(r)$ , e.g.  $Q(0)$  is solely determined by  $ka$ . For this reason with given  $k$  and  $a$  parameters by taking  $q(r) \equiv 0$  we can try to calculate the approximate bound states or at least estimate their number. In what follows we show exact results for the constant  $q$ -potential, which case contains the zero  $q$ -potential case as well.

For  $Q(x) = -se^{-2tx}$  with  $s, t > 0$  the Sturm Liouville equation can be solved explicitly. This is an easy exercise and will not be detailed here, only the result is given. The differential equation

$$-\psi''(x) - se^{-2tx}\psi(x) = \lambda\psi(x) \quad (79)$$

is solved by

$$\psi(x) = C_1 J_{i\sqrt{\lambda}/t} \left( \frac{\sqrt{s}}{t} e^{-tx} \right) + C_2 J_{-i\sqrt{\lambda}/t} \left( \frac{\sqrt{s}}{t} e^{-tx} \right) \quad (80)$$

where Bessel functions generally of complex orders have appeared. For  $\text{Im}\sqrt{\lambda} > 0$  the  $L^2$ -solution (if  $t > 0$ ) is

$$\psi(x) = C_2 J_{-i\sqrt{\lambda}/t} \left( \frac{\sqrt{s}}{t} e^{-tx} \right), \quad (81)$$

since

$$J_{\pm i\sqrt{\lambda}/t} \left( \frac{\sqrt{s}}{t} e^{-tx} \right) = b(x) x^{\mp \text{Im}\sqrt{\lambda}/t} + o(x^{\mp \text{Im}\sqrt{\lambda}/t}), \quad x \rightarrow 0, \quad (82)$$

where  $b(x)$  is a bounded function. Then the m-function is

$$m(\lambda) = \frac{\psi'(0)}{\psi(0)} = -\sqrt{s} \frac{J'_{-i\sqrt{\lambda}/t}(\sqrt{s}/t)}{J_{-i\sqrt{\lambda}/t}(\sqrt{s}/t)}. \quad (83)$$

Using the Stieltjes inversion, equation (29),  $d\rho^h(\lambda)$  can be found. For  $\lambda > 0$  trivially

$$d\rho^h(\lambda) = \frac{1}{\pi} \text{Im} \left[ \sqrt{s} \frac{J'_{-i\sqrt{\lambda}/t}(\sqrt{s}/t)}{J_{-i\sqrt{\lambda}/t}(\sqrt{s}/t)} + h \right]^{-1} d\lambda, \quad \lambda > 0. \quad (84)$$

For  $\lambda < 0$  the measure is concentrated to points which are the bound states. They are located at the eigenvalues of the operator where  $\psi \in L^2(0, \infty)$ . Starting from  $\psi(0) = 1$  and  $\psi'(0) = h$  one can calculate the coefficient of the diverging solution to be

$$C_1 = -\frac{\pi\sqrt{s}}{2t} \left[ J'_{\sqrt{-\lambda}/t}(\sqrt{s}/t) + \frac{h}{\sqrt{s}} J_{\sqrt{-\lambda}/t}(\sqrt{s}/t) \right] \quad (85)$$

where some elementary properties of the Bessel functions were used [8].  $C_1$  needs to be zero thus the bound states are located at  $\lambda$ 's that satisfy

$$J'_{\sqrt{-\lambda}/t}(\sqrt{s}/t) + \frac{h}{\sqrt{s}} J_{\sqrt{-\lambda}/t}(\sqrt{s}/t) = 0. \quad (86)$$

Note that the number of bound states is greater than zero but finite.

Using the theory of residues the height of the step in  $\rho(\lambda)$  at the bound states can be obtained to be

$$\rho(\lambda_0 + 0) - \rho(\lambda_0 - 0) = 2t\sqrt{-\lambda} \frac{J_{\sqrt{-\lambda_0}/t}(\sqrt{s}/t)}{\sqrt{s} J_{\sqrt{-\lambda_0}/t}^{(1,1)}(\sqrt{s}/t) + h J_{\sqrt{-\lambda_0}/t}^{(1,0)}(\sqrt{s}/t)}, \quad (87)$$

where the superscript  $(n, m)$  means derivation with respect to order  $n$  times and derivation with respect to the variable  $m$  times.

In case of  $h = 0$  we have a particularly simple scenario at hand. For definiteness let

$$\kappa^2 = k^2 - q(0) \quad (88)$$

Table 1: The first few sectors of definite bound state numbers for a constant  $q(r)$  potential at  $h = 0$ .

$0 < \kappa a < 3.8317$	one bound state
$3.8318 < \kappa a < 7.0156$	two bound states
$7.0156 < \kappa a < 10.174$	three bound states
$10.174 < \kappa a < 13.324$	four bound states
	etc.

( $q(0)$  being the value of the constant potential at the origin, and suppose for simplicity that  $q(0) < k^2$ ). The potential  $Q(x) = -\frac{(\kappa a)^2}{c^2}e^{-\frac{2x}{|c|}}$  with  $h = 0$  has bound states  $\lambda_i$  at

$$J'_{|c|\sqrt{-\lambda_i}}(\kappa a) = 0. \quad (89)$$

From [8] we infer, denoting the  $n$ th root of  $J'_\mu(x)$  by  $j'_{\mu,n}$ , that  $j'_{\mu,n} < j'_{\mu+\varepsilon,n}$   $n = 1, 2, \dots$  holds with  $j'_{0,1} = 0$ . Moreover,  $j'_{\mu,n}$  is continuous in  $\mu$  [8]; therefore, we find that for  $\kappa a > 0$  there always exists at least one bound state. From the above fact it also follows that the number of zeros of  $J'_0(x)$  on  $0 \leq x < \kappa a$  equals the number of bound states of  $Q(x) = -\frac{(\kappa a)^2}{c^2}e^{-\frac{2x}{|c|}}$ . Alternatively, as  $J'_0(x) = -J_1(x)$ , the number of bound states increase at the zeros of  $J_1(x)$ , i.e. at  $j_{1,n}$ ,  $n = 1, 2, \dots$ . Some numerical results are listed in Table 1. For a general potential  $q(r)$  the data listed in Table 1 can still be relevant if the potential is shallow compared to  $k^2$  and only the tail of  $Q(x)$  is influenced by  $q(r)$ . Note that the value of the parameter  $c$  does not affect the number of bound states (only their positions) as it is only a scale parameter of the function  $J'_{|c|\sqrt{-\lambda}}(\kappa a)$  of  $\sqrt{-\lambda}$  whose zeros give the bound states.

Allowing  $h \neq 0$  gives rise to the more involved condition (86) for the bound states. It is possible then for some  $h \neq 0$  that one has one bound state while for  $h = 0$  two of them. This has the favorable consequence of reducing a nonlinear problem to a linear one. Without giving an exhaustive treatment of the situation we show the following illustrative result for bound state reduction.

**Lemma 1.** *For  $3.83 \approx j'_{0,2} < \kappa a < j_{0,2} \approx 5.52$  the two bound states present at  $h = 0$  can be reduced to one by varying  $h$ .*

*Proof.* In figure 1 the two Bessel-type functions entering condition (86) are depicted. We will show that by varying  $h$  (on the figure through  $R$ ), disregarding an overall sign, one can always get the same kind of graphs as the ones on the figure.

By using the fact that the zeros of  $J_0(x)$  and  $J'_0(x)$  interlace we infer  $J_0(\kappa a) \neq 0$  and  $J'_0(\kappa a) \neq 0$ . The only thing that remains to be shown is that the distribution of the zeros are as depicted. Since  $j'_{0,2} < \kappa a < j_{0,2}$  for  $J'_k(\kappa a)$  only the first two and for  $J_k(\kappa a)$  only the first zeros can enter our considerations. Then the interlacing relation  $j'_{a,1} < j_{a,1} < j'_{a,2}$  translates to  $k_1 < k_2 < k_3$  if  $j'_{k_1,1} = \kappa a$ ,  $j_{k_2,1} = \kappa a$  and  $j'_{k_3,2} = \kappa a$ . This completes the proof of the lemma.  $\square$

## 6 Examples

### 6.1 Reconstruction of constant potentials

First we reconstruct a potential

$$q(r) = \begin{cases} 1.2 & \text{for } r \leq 2 = a \\ 0 & \text{for } r > 2 = a \end{cases} \quad (90)$$

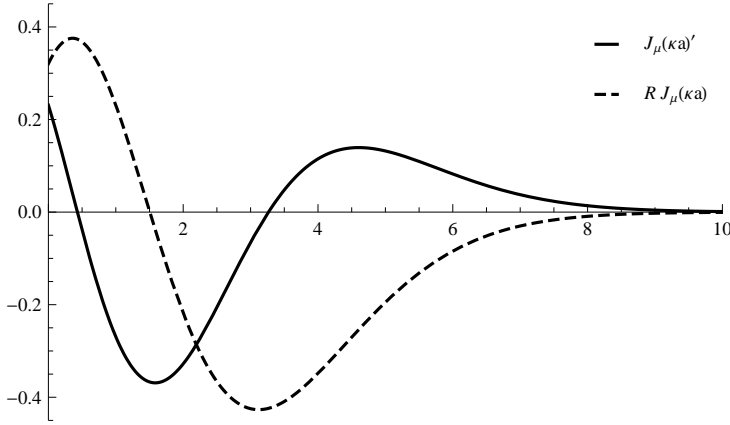


Figure 1:  $J_\mu(\kappa a)'$  (full line) and  $RJ_\mu(\kappa a)$  (dashed line) as functions of the order ( $R$  is a real number satisfying  $\text{sgn}(J'_0(\kappa a)) = \text{sgn}(RJ'_0(\kappa a))$  and  $|RJ_0(\kappa a)| > |J'_0(\kappa a)|$ ). While at  $h = 0$  the zeros of the derivative functions are the bound states, at  $h \neq 0$  the intersection of the two graphs give them.

at  $k = 1$  that generates no bound states in the auxiliary problem (because  $Q(x) > 0$ ).

Figure 2<sup>1</sup> shows the quality of the reconstructions when 5, 10, 20 and 40 input phase shifts are used with the standard choice of parameters ( $c = -1$ ,  $h = 0$ ). As expected we see that the quality of the inversion procedure gets better as the number of input data is growing.

We may let the parameters  $c$  and  $h$  change from the standard values and prescribe the smoothness of the inverse potential  $q(r)$ . This can be done by monitoring the quantity

$$s(c, h) = \int_{r_0}^a |q'(r)| dr \quad (91)$$

at each values of the parameters  $c$  and  $h$  where the lower limit  $r_0$  is introduced in order to exclude (possible pathological) singularity at the origin. Note that we used  $r_0 = 0.05$  in all the examples shown. By requiring  $s$  to be small is equivalent to exclude nonphysical potentials (see also [11]). On the other hand, this requirement also means that we encounter smooth  $F$ -functions too, in agreement with Theorem 1.

Figure 3 shows that choosing a modest number  $N = 10$  of input data we also get excellent reconstruction when  $s$  is small. The optimal choice of parameters has proved to be  $c = -0.3$  and  $h = -0.15$  (3(d)).

Several other techniques can also be employed to find optimal results. One is to retain the constant term  $c_0$  in the expansion (49). The value of  $c_0$  (i.e. the departure from zero) serves also as an overall indicator of the accuracy of the procedure. Another trick is to reconstruct the potential using the one bound state procedure, that is by retaining the  $c_{-1} = b/2$  term and the associated nonlinear parameter  $\sqrt{-\lambda}$  (a possible spurious bound state). This procedure also affects beneficently the numerics and can be applied both in the zero and one bound state cases.

In Table 2 we list the input phase shifts  $\delta_l$  and the intermediate data (moments  $\mu_l$ , coefficients  $c_n$  and the value  $\sqrt{-\lambda}$ ) of the inverse calculation with  $c = -0.3$  and  $h = -0.5$  (where  $s = 0.0004$ ). As we see the procedure yields  $\sqrt{-\lambda} = -1.4447$  for the "bound state" parameter, a negative value which clearly indicates that there is no true bound state in the auxiliary problem.

---

<sup>1</sup>For brevity of the figure captions we introduce the function  $H_a(x)$  being a step function:  $H_a(x) = 1$  for  $x \leq a$  and  $H_a(x) = 0$  for  $x > a$ .

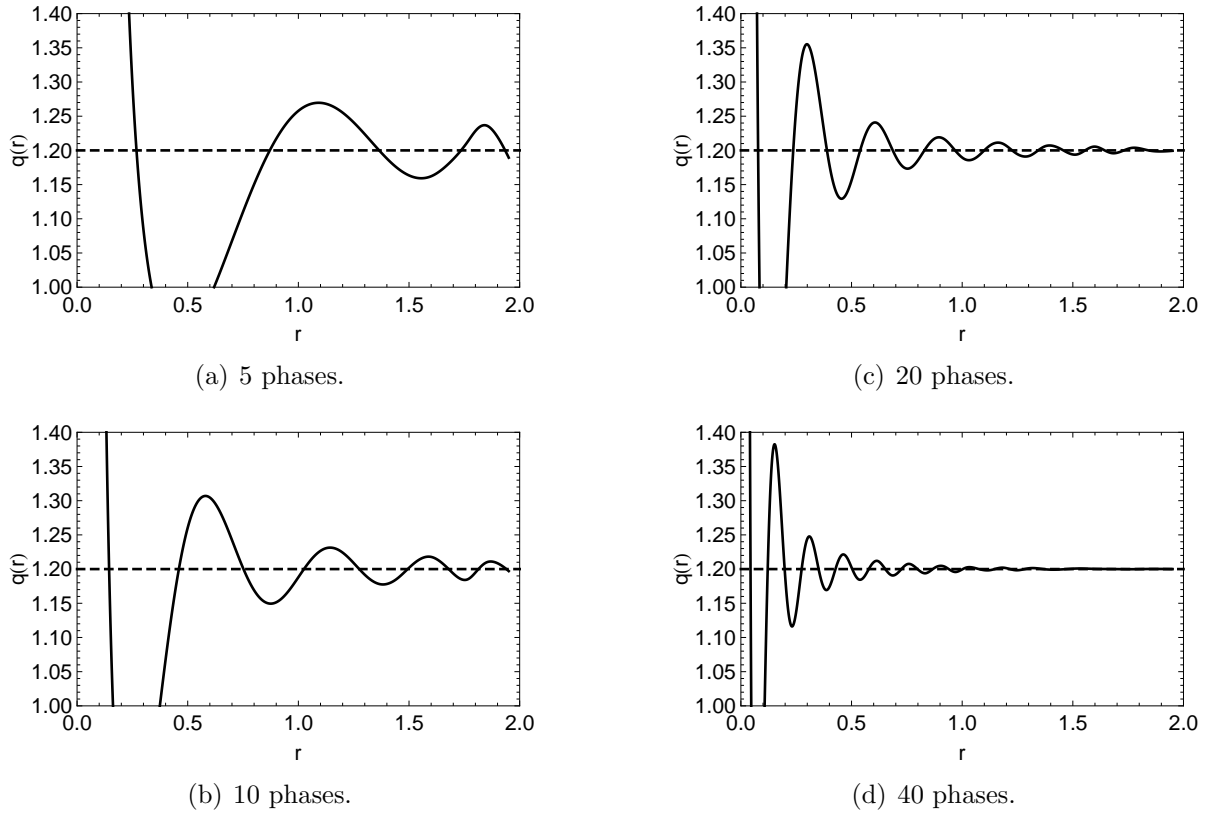


Figure 2: Reconstructions with different number of input phase shifts of the constant potential  $q(r) = 1.2 H_2(r)$ . ( $c = -1$ ,  $h = 0$ .)

Now we proceed to reconstruct the potential

$$q(r) = \begin{cases} 0.8 & \text{for } r \leq a \\ 0 & \text{for } r > a \end{cases} \quad (92)$$

at  $k = 1$  that generates one auxiliary bound state with  $a = 2$  and two auxiliary bound states with  $a = 11$  (choosing  $h = 0$ ).

Figure 4(a)-(b) shows that the inversion procedure yields a better potential for the smaller  $s$  value also in this one (auxiliary) bound state case. The deviation of the inverse potential from the original one in the region  $0.5 < r < 2$  is of the order of 0.00010 for  $s = 0.049$  (at  $c = -1$ ,  $h = 0$ ) and 0.00005 for  $s = 0.0022$  (at  $c = -0.5$ ,  $h = -0.65$ ).

Figure 4(c)-(d) shows two reconstructions in the case when two bound states exist in the auxiliary problem. In the first case (figure 4(c)) the inverse potential is obtained by the use of the two bound state method with parameters  $c = -1.5$ ,  $h = 0$  and finding the nonlinear (bound state) parameters at  $\lambda_1 \approx -0.48$ ,  $\lambda_2 \approx -2.43$  (starting from the trial values of  $\lambda_1 \approx -0.8$ ,  $\lambda_2 \approx -2.3$ ). In the second case (figure 4(d)), the inverse potential has been calculated by using the one bound state procedure with the parameters choice  $c = -1$ ,  $h = 5$  (providing for the bound state parameter the value  $\lambda = -2.41$ ). We see that both methods yield similar results. However, while the two bound state calculation needs an a priori guess about the positions of the auxiliary bound states, the one bound state method does not suffer from such an ambiguity and the calculation can be performed in the linear regime. One can check that in this case  $\kappa a \approx 4.92$ , thus we are in the domain where the number of bound states can be reduced (Lemma 1) by varying  $h$ .

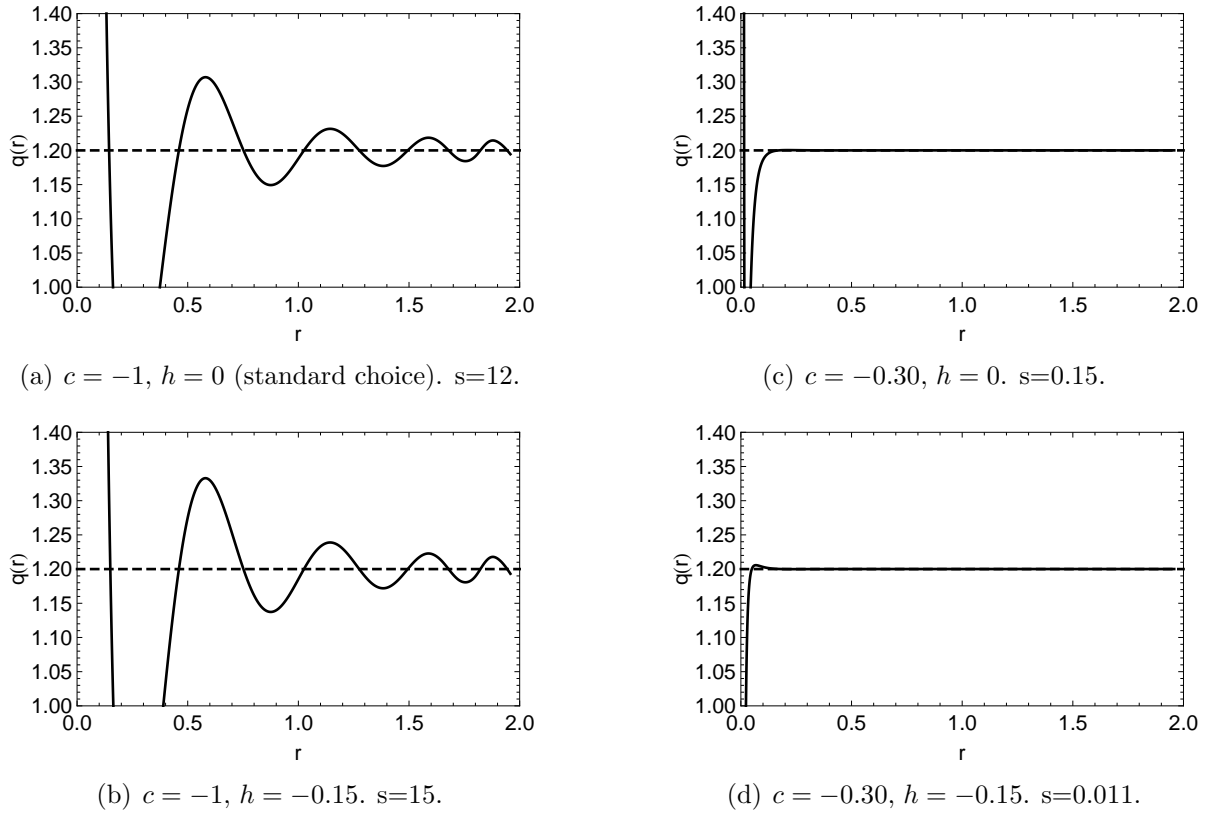


Figure 3: Reconstructions with different choices of the parameters of the constant potential  $q(r) = 1.2 H_2(r)$  from 11 phase shifts with no bound states in the auxiliary problem.

## 6.2 Reconstruction of potentials with different shapes

Figure 5(a)-(b) shows the reconstruction of the two potentials given by

$$q_{\text{Gauss}}(r) = -4e^{-5r^2}, \quad q_{\text{WS}}(r) = -\frac{4}{1 + e^{\frac{r-0.5}{0.1}}}. \quad (93)$$

The reconstructions have been carried out at  $k = 1.5$  with 7 input phase shifts given with a precision of 4 digits for the Gauss potential  $q_{\text{Gauss}}(r)$ , and with 4 input phase shifts given with a precision of only 2 digits for the Woods-Saxon shaped potential  $q_{\text{WS}}(r)$ . In both cases the one bound state approximation procedure is applicable. For the Gauss potential the reconstruction with the parameters  $a = 1.5, c = -0.74$ , and  $h = 0$  resulted in the bound state position at  $\lambda = -3.36$ . Note that this figure agrees with the exact bound state position (when calculated from the known auxiliary potential  $Q(x)$ ) and only slightly differs from the assessed value of  $\lambda = -3.22$  (calculated from equation (89)). For the WS potential the reconstruction was carried out with the parameters  $a = 2, c = -1.25, h = 0$  and resulted in the bound state position at  $\lambda = -2.46$  to be compared with the assessed value of  $\lambda = -2.44$ .

## 6.3 Inverse potentials from experimental phase shifts

### 6.3.1 $e - Ar$ atom scattering at $E = 12$ eV (0.4412 au).

The experimental phase shifts derived by Williams [12] from  $e - Ar$  scattering experiment at  $E_{\text{c.m.}} = 12$  eV and the inversion parameters  $a$  and  $c$  are listed in the first line of Table 3. At  $c = -3.7$  and  $h = 1.9$  the bound state parameter was found to be  $\lambda = -0.44$ . The resulted potential of the HA calculation is shown by the continuous line in Fig. 6(a) and compared with that obtained by the modified Newton-Sabatier (mNS) inversion method [13] (dashed curve).

Table 2: Input phases  $\delta_l$  and the intermediate quantities of the inversion procedure of the potential  $q(r) = 1.2 H_2(r)$ : moments  $\mu_l$ , coefficients  $c_n$  and the nonlinear parameter (i.e. 'bound state').

$l$	$\delta_l$	$\mu_l$	$n$	$c_n$
0	-0.9890	-0.1714	-1	-6.4667 <sup>a</sup>
1	-0.2964	-0.0043	0	+0.0002
2	-0.0471	0.0151	1	-0.0954
3	-0.0037	0.0180	2	+7.2085
4	-0.0001	0.0176	3	-0.1510
5	$-5.0 \times 10^{-6}$	0.0164	4	+0.2657
6	$-1.1 \times 10^{-7}$	0.0151	5	-0.2968
7	$-1.8 \times 10^{-9}$	0.0139	6	+0.2027
8	$-2.2 \times 10^{-11}$	0.0129	7	-0.2022
9	$-2.3 \times 10^{-13}$	0.0119	8	+0.0258
10	$-1.9 \times 10^{-15}$	0.0111	9	+0.0092

<sup>a</sup> Nonlinear "bound state" parameter:  $\sqrt{-\lambda} = -1.4447$ .

Table 3: Input phase shifts  $\delta_l$  derived from  $e - Ar$  and  $n - \alpha$  scattering experiments performed at one and three centre of mass energies, respectively. Corresponding inversion parameters  $c$  and  $a$ .  $h = 1.9$  was used in case of the  $e - Ar$  inversion while  $h = 0$  was taken for the three  $n - \alpha$  inversions.

$E_{\text{c.m.}}$	$\delta_0$	$\delta_1$	$\delta_2$	$\delta_3$	$a$	$c$
12 (eV)	-1.218	-0.626	1.191	0.118	3.9	-3.70
9.6 (MeV)	1.763	1.553	0.028		3.9	-4.25
12.8 (MeV)	1.676	1.466	0.066		3.4	-2.96
16.0 (MeV)	1.588	1.396	0.117		3.3	-2.37

Both potentials compare well showing the usability of the present method. The  $e - Ar$  potential has an attractive part with a minimum value of about  $-2.8$  au at a distance of  $r \approx 1.2$  au. At smaller distances the potential is of repulsive nature which can be interpreted as a manifestation of the Pauli-principle. Further details can be found in Ref. [14].

### 6.3.2 $n - \alpha$ particle scattering.

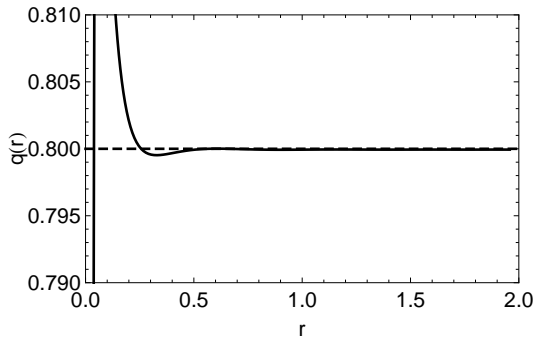
Input data at energies  $E_{\text{c.m.}} = 9.6, 12.8$ , and  $16.0$  MeV are listed in the lower three lines of Table 3 together with the inversion parameters  $a$  and  $c$ . The input phase shifts are taken from the comprehensive analysis of the  $n - \alpha$  scattering presented by Ali et al [15]. Because of the spin-orbit coupling both spin-up  $\delta_l^+$  and spin-down  $\delta_l^-$  phase shifts contribute to the scattering amplitude at each partial wave. In case of weak spin-orbit coupling (which is assumed) the combined phase shifts

$$\delta_l = \frac{1}{2l+1}[(l+1)\delta_l^+ + l\delta_l^-] \quad (94)$$

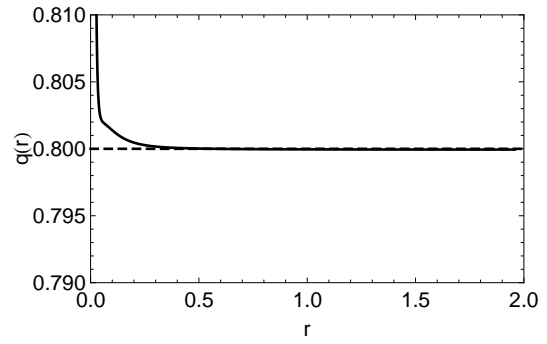
are characteristic of the underlying central potential [16], and these data are used as input for the HA procedure.

The resulting three HA potentials are exhibited in Fig. 6(b). As we see they offer a similar physical interpretation for the scattering process as before in the case of electron-inert gas

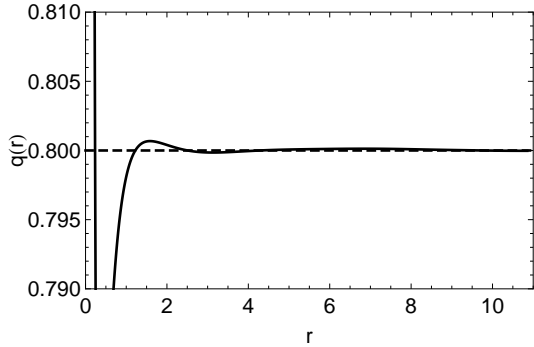




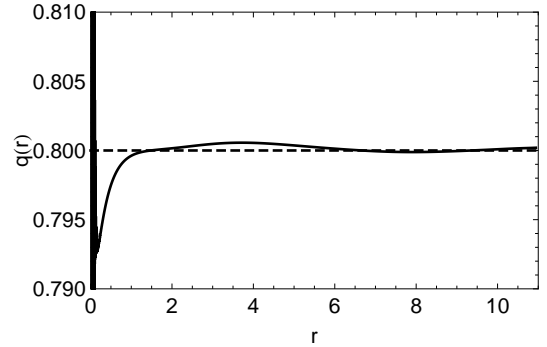
(a)  $c = -1.0$ ,  $h = 0$ ,  $\lambda = -0.105$ ,  $s = 0.049$ .



(b)  $c = -0.5$ ,  $h = -0.65$ ,  $\lambda = -1.39$ ,  $s = 0.0022$



(c)  $c = -1.5$ ,  $h = 0$ ,  $\lambda_1 = -0.48$ ,  $\lambda_2 = -2.43$ ,  $s = 1.28$ , two bound states.



(d)  $c = -1.5$ ,  $h = 5$ ,  $\lambda = -2.41$ ,  $s = 0.11$ , one bound state.

Figure 4: (a)-(b) Reconstructions of the constant potential  $q(r) = 0.8 H_2(r)$  from 11 phase shifts and one bound state in the auxiliary problem at  $h = 0$  with different choices of the parameters. (c)-(d) Reconstructions of the potential  $q(r) = 0.8 H_{11}(r)$  using (c) the two bound state formulation ( $h = 0$ ) and (d) the one bound state method ( $h = 5$ ). The constant term was present in (49) during the calculation.

atom collision: the approaching colliding partners, neutron and alpha particle are attracting each other when entering the domain of nuclear forces. The attraction is culminating around the  $\alpha$ -particle surface between  $r \approx 1.1 - 1.2$  fm, reaching a strength of potential energy between  $-50$  and  $-52$  MeV. When the colliding partners are merging the Pauli repulsion (originating from the fermionic exchange) takes into effect and this is overcome by the nucleonic soft core repulsion at very small distances at  $r \approx 0.1 - 0.2$  fm. Because the resulting inversion potentials are also very similar at these different energies between  $9 - 16$  MeV, we may have found the energy-independent potential responsible for the scattering data which is always the desirable goal of any fixed energy inversion procedure.

## 7 Conclusions

We have surveyed, developed further and applied the constructive inverse scattering method of Horváth and Apagyi (HA) [4]. The inverse problem consists of finding a scattering potential of finite support in the radial Schrödinger equation from a finite number of scattering phase shifts given at one fixed energy. The solution procedure consists of solving an auxiliary inverse spectral problem of the classical Sturm-Liouville equation whose spectral data is determined by the phase shifts of the fixed energy inverse scattering problem. The auxiliary inverse spectral problem is equivalent to a moment problem.

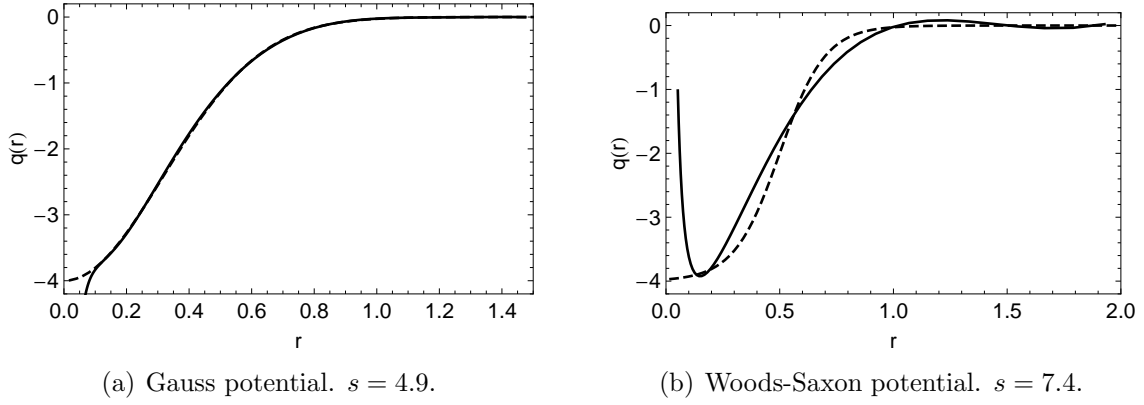


Figure 5: Reconstruction of potentials with different shapes. (a) Gaussian shape from 7 phase shifts, (b) Woods-Saxon shape from 4 phase shifts. The original potential is depicted with dashed line while the reconstruction is illustrated with solid line. For parameters and accuracy see the text.

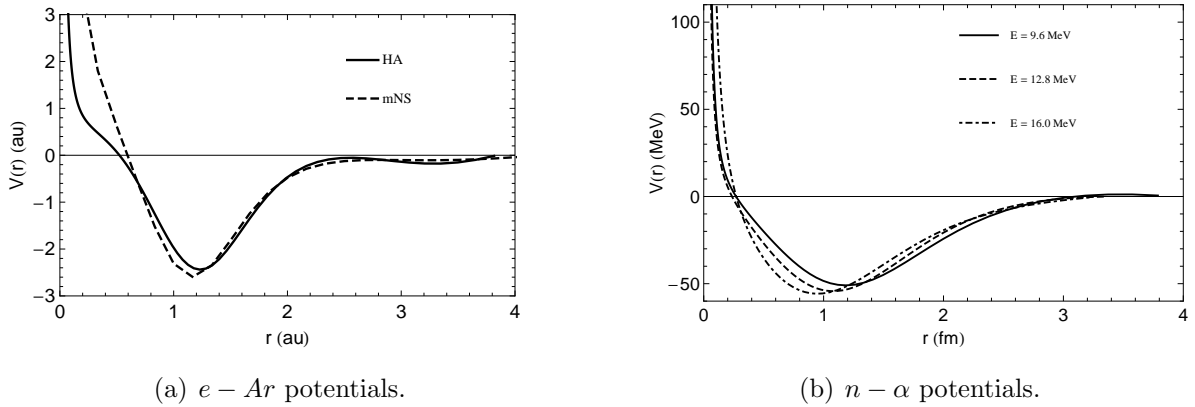


Figure 6: Construction of potentials from experimental phase shifts listed in Table 3. (a) HA (continuous line) and mNS (dashed line) inverse potentials for  $e - Ar$  scattering at 12 eV. (b) Inverse potentials for  $n - \alpha$  scattering at three c.m. energies of 9.6, 12.8, and 16.0 MeV.

The HA method has been developed further in that two hidden parameters of the theory have been disclosed and enabled to vary. One of these parameters is a scale parameter  $c$  appearing in the Liouville transformation. It plays an important role in the solution of the moment problem. The other parameter is an initial value parameter  $h$  which enters the Gel'fand-Levitan constructive inversion scheme. The hidden (also called standard) values of these parameters have been  $c = -1$  and  $h = 0$ . By making these parameters free the HA method proves to be applicable to cases where only a limited precision of input data is expected as in the case of the inversion of phase shifts derived from measured cross sections.

Depending on the number of bound states present in the auxiliary inverse spectral problem, various solution methods of the moment problem have been presented and applied to calculate the potential from a set of given phase shifts which can be either calculated theoretically if the underlying potential is known (reconstruction procedure) or derived, e.g. from collision experiments if the potential is not known (construction procedure). Of course, an inverse method aims at solving the latter task, and the prior one may serve for testing or developing further the procedure.

The examples illustrate that a dramatic improvement of the HA inversion method can be achieved by the proper adjustment of the parameters  $c$  and  $h$ . We may, for example,

reduce the number of bound states of the auxiliary inverse spectral problem by one. Because the most sensitive part of the method is the possible presence of auxiliary bound states we have established a procedure to assess their number. This procedure is based on the free motion because only the asymptotical part of the auxiliary potential is influenced by the wanted fixed energy potential. Alternatively, one may also use other (less sophisticated) fixed energy inverse scattering methods, e.g. the modified Newton-Sabatier procedure [13], to assess the number of auxiliary bound states. By using an independent phase equivalent method, one can simultaneously check the inverse potential provided by the HA procedure.

Finding an optimal choice of the parameters  $a$ ,  $c$ , and  $h$  can proceed through satisfying physical arguments. For example, one can obtain a cheap calculation (that is using small number of input data) via prescribing a maximal smoothness for the inverse potential. With such a prescription we have reproduced known potentials. Another (or simultaneous) prescription can be to check the inverse potential whether it fulfills the approximate relation  $V(a) \approx 0$ . With this prescription we have got the inverse potentials equivalent to the measured phase shifts of  $e - Ar$  and  $n - \alpha$  scattering experiments. Note that by making the parameters  $c$  and  $h$  flexible one may also avoid the appearance of non-physical (e.g. singular) inverse potentials [11] which can arise e.g. when the solution of the GL equation is not unique.

The HA method can be extended into various directions. A natural extension is to develop the theory to handle complex phase shifts which describe inelastic processes. Another extension would be to efficiently treat Coulombic processes, i.e. charged particle scattering. An interesting and important extension would be an alternative formulation where the auxiliary spectral problem is solved by the Marchenko integral equation [17]. The latter development is in progress.

## Acknowledgements

The authors thank Professor Miklós Horváth for valuable discussions and for reading the manuscript.

## References

- [1] Newton R G 2002 *Scattering Theory of Waves and Particles: Second Edition* (Dover Publications)
- [2] Chadan K, Sabatier P C 1977 *Inverse Problems in Quantum Scattering Theory* (New York, USA: Springer-Verlag)
- [3] Horváth M 2006 *Trans. Amer. Math. Soc.* **358** 5161
- [4] Horváth M, Apagyi B 2008 *Mod. Phys. Lett. B* **22** 2137
- [5] Birkhoff G, Rota G C 1989 *Ordinary differential equations* (New York, USA: Wiley)
- [6] Levitan B M 1987 *Inverse Sturm-Liouville problems* (Utrecht, the Netherlands: VNU Science Press)
- [7] Levitan B M, Sargsyan I S 1975 *Introduction to spectral theory: selfadjoint ordinary differential operators* (Amer. Math. Soc., translated from Russian)
- [8] Watson G N 1922 *A treatise on the theory of Bessel functions* (Cambridge, UK: Cambridge University Press)

- [9] Schechter S 1959 *Math. Tab. and Other Aids of Comp.* **13** 73
- [10] Talenti G 1987 *Inverse Problems* **3** 501
- [11] Pálmai T and Apagyi B 2010 *J. Math. Phys.* **51** 022114
- [12] Williams J F 1979 *J. Phys. B: At. Mol. Phys.* **12** 265
- [13] Münchow M and Scheid W 1980 *Phys. Rev. Letters* **44** 1299
- [14] Apagyi B, Lévy P, and Scheid W 1997 *Lecture Notes in Physics* **488** 156
- [15] Ali S, Ahmad A A Z and Ferdous N 1985 *Rev. Mod. Phys.* **57** 923
- [16] Leeb H, Huber H and Fiedelhey H 1995 *Phys. Lett. B* **344** 18
- [17] Marchenko V A 2011 *Sturm-Liouville operators and applications* (Amer. Math. Soc.)